Pseudoscalar quarkonium+γ production at NLL+NLO accuracy

Hee Sok Chung,[a] **June-Haak Ee,**[b] **Daekyoung Kang,**[c] **U-Rae Kim,**[b] **Jungil Lee**[b] **and Xiang-Peng Wang**[c]

[a]*Physik Department, Technische Universität München,*
James-Franck-Str. 1, D-85748 Garching, Germany

[b]*Department of Physics, Korea University,*
Seoul 02841, Korea

[c]*Key Laboratory of Nuclear Physics and Ion-beam Application (MOE) and*
Institute of Modern Physics, Fudan University,
Shanghai, China 200433

E-mail: heesok.chung@tum.de, chodigi@gmail.com, dkang@fudan.edu.cn, sadafada@korea.ac.kr, jungil@korea.ac.kr, xiang.peng.wang@desy.de

ABSTRACT: We consider the exclusive pseudoscalar heavy-quarkonium ($\eta_{b,c}$) production in association with a photon at future lepton colliders where the collider energies of $O(10^2)\,\mathrm{GeV}$ are far greater than the quarkonium mass. At these energies, the logarithm of mass to collision energy becomes increasingly large hence its resummation becomes particularly important. By making use of the light-cone-distribution factorization formula, we resum the logarithms up to next-to-leading-logarithmic accuracy (NLL) that corresponds to order-α_s accuracy. We combine the resummed result with a known fixed-order result at next-to-leading order (NLO) such that both resummed-logarithmic terms and non-logarithmic terms are included at the same order in α_s. This allowed us to provide reliable predictions at accuracies of order α_s ranging from relatively low energies near quarkonium mass to the collider energies of $O(10^2)\,\mathrm{GeV}$. We also include the leading relativistic corrections resummed at leading-logarithmic accuracy. Our prediction at the Belle energy is comparable with fixed-order predictions in literatures while it shows a large deviation from a recent Belle's upper limit by about $4\,\sigma$. Finally, we make predictions for the energies of future Z- and Higgs factories.

KEYWORDS: QCD Phenomenology

ARXIV EPRINT: 1906.03275

Contents

1 Introduction

Rigorous quantitative understanding of the heavy-quarkonium production at high-energy colliders [1] is a key probe not only to the features of quantum chromodynamics (QCD) but also to fundamental phenomena such as quark-gluon plasma (QGP) in heavy-ion collisions [2] and heavy-quark Yukawa couplings to Higgs [3, 4]. An effective field-theoretic framework called the nonrelativistic QCD (NRQCD) [5] can be employed to predict quarkonium productions at high-energy colliders in a systematic way. NRQCD describes the dynamics inside a quarkonium at the energy scale $m_Q v^2$, where m_Q is the mass of the heavy quark Q and v is the relative velocity of the Q and $\bar{Q}$ in the bound state. NRQCD is blind to the short-distance dynamics at higher energy scales of order $\gtrsim m_Q$ and the corresponding short-distance coefficients can be determined by matching to the full theory, QCD, which is known to be correct in all accessible energy scales. As a result, the production cross sections or decay rates involving heavy quarkonia can be expressed as linear combinations of NRQCD long-distance matrix elements (LDME) with the short-distance coefficients.

Exclusive processes such as associated photon production or double-quarkonium production at the lepton colliders like B factories and BES have been extensively studied in

the framework of NRQCD. Future lepton colliders such as ILC [6], CEPC [7], and FCC-ee [8] offer opportunities to test our understanding of their productions at higher energies of $O(10^2)\,\text{GeV}$. In a collision at such a large center-of-momentum (CM) energy $\sqrt{s}$, the cross section of a quarkonium has an uncomfortably strong dependence on the large logarithm of the ratio

$$r \equiv \frac{4m_Q^2}{s}. \tag{1.1}$$

A straightforward extrapolation of the prediction for a lower-energy process of $\sqrt{s} \lesssim 10\,\text{GeV}$ to higher-energy processes listed above may result in a failure of predictive power. Thus the accuracy of a prediction can be reasonably controlled only after resumming the large logarithmic contributions in a proper way because such a logarithm cannot be suppressed by the strong coupling constant:

$$\alpha_s \ln r \sim O(1).$$

The resummation of such a logarithm can be made by employing the light-cone (LC) approach [9, 10] or, equivalently, the soft-collinear effective theory (SCET) [11]. In SCET, the scattering amplitude or current-current correlator is factorized into the following factors: the hard-scattering kernel involving scales of $\sqrt{s}$, the light-cone distribution amplitude (LCDA) that represents the collinear part, and the decay constant that involves the interactions of scales $\lesssim m_Q$. By solving the renormalization-group (RG) equation for collinear part or the hard part, one can resum the logarithms $\ln r$.

In general, the collinear part describing a light meson such as a pion, ρ, or η is nonperturbative and one usually introduces an LCDA with a few model parameters. However, in the case of heavy quarkonium, the collinear parts can further be factorized into perturbative short-distance coefficients at the scale m_Q and nonperturbative long-distance matrix elements at the scale $m_Q v^2$ in the framework of NRQCD [12–15]. Therefore, it is worth to revisit and to update predictions by including the resummation of the large logarithms at energies of future lepton colliders. We express our formula in such a way that our expression reproduces the fixed-order results at low energies $\sim m_Q$, and at higher energies it resums large logarithms so that the same expression can be used for both the Belle and future high-energy experiments.

We consider the charge conjugate even ($C = +1$) processes with S-wave pseudoscalar quarkonium such as $\eta_c + \gamma$ and $\eta_b + \gamma$. In a fixed-order perturbation theory this process was first computed in [16] at leading order (LO) and its next-to-leading order (NLO) correction was computed analytically in [17, 18] and numerically in [19]. Up to date the α_s^2 correction is available [20, 21]. The relativistic correction of the order v^2 was first considered in [22] and $\alpha_s v^2$ correction was also obtained in [23]. The virtual Z contribution was computed up to α_s correction in [24, 25].

The leading-logarithmic (LL) accuracy resumming $\alpha_s^n \log^n r$ terms was first achieved in [12]. The quarkonium LCDAs at NLO were obtained by matching QCD onto NRQCD in [14, 15]. In Higgs or Z boson decay into $J/\psi + \gamma$ processes [26–29], the next-to-leading-logarithmic (NLL) accuracy resumming $\alpha_s^{n+1} \log^n r$ was achieved and the Abel-Padé method which enables to handle divergences appearing in computing the relativistic

correction to the rates, was developed as well. Using the method, we make the prediction for $\eta_{c,b} + \gamma$ in lepton colliders at NLL+NLO plus the leading v^2-correction accuracy.

The rest of the paper is organized as follows. In section 2 we explain the theoretical formula to achieve NLL+NLO accuracy and provide all the ingredients for that order. Section 3 presents numerical results for the cross section and for the Z-boson decay rate into this process and section 4 compares our result at the Belle energy to the previous results and to Belle's recent limit [30]. We finally summarize in section 5.

2 Theoretical formula

The LC approach allows us to capture and to resum all logarithmic terms (singular), while non-logarithmic terms (nonsingular) can be computed by NRQCD fixed-order perturbation theory. We can express our full cross section as a sum of singular and nonsingular parts as in [31, 32].

$$\sigma(r; \mu, \mu_0, \mu_{\mathrm{ns}}) = \sigma^{\mathrm{sing}}(r; \mu, \mu_0) + \sigma^{\mathrm{ns}}(r, \mu_{\mathrm{ns}}), \qquad (2.1)$$

where sing and ns in the superscripts and subscripts denote singular and nonsingular, respectively. In the singular part the scattering amplitude is factorized into a hard scattering kernel, an LCDA, and an NRQCD LDME. Each of them depends on a relevant energy scale such as $\mu \sim \sqrt{s}$, or $\mu_0 \sim m_Q$.[1] The renormalization group (RG) evolution between those scales enables us to resum large logarithms appearing in the fixed-order cross section and details of the evolution will be presented in coming subsections. On the other hand, if we turn off the resummation by setting all the scales being the same, it reduces to the singular part of the fixed-order cross section: $\sigma^{\mathrm{fixed\text{-}sing}}(r; \mu) = \sigma^{\mathrm{sing}}(r; \mu, \mu)$. The singular part of fixed-order cross section is given by

$$\sigma^{\mathrm{fixed\text{-}sing}}(r; \mu) = \lim_{r \to 0} \sigma^{\mathrm{fixed}}(r; \mu) = \sigma_0 \left[1 + \frac{\alpha_s C_F}{4\pi} c^{\mathrm{sing}} + \langle v^2 \rangle c_{v^2}^{\mathrm{sing}} \right], \qquad (2.2)$$

where the coefficients are[2]

$$\begin{aligned} c^{\mathrm{sing}} &= -\frac{2}{3} \left[(9 - 6\log 2)\log r + 9(3 + \log^2 2 - 3\log 2) + \pi^2 \right], \\ c_{v^2}^{\mathrm{sing}} &= -\frac{4}{3}. \end{aligned} \qquad (2.3)$$

The born cross section σ_0 is given by

$$\sigma_0 = \frac{16\pi^2 \alpha^2(\sqrt{s})\alpha(0)e_Q^2 \tilde{e}_Q^2 m_P}{3s^2} \frac{\langle \mathcal{O}_1 \rangle_P}{m_Q^2}, \qquad (2.4)$$

---

[1]There is the non-perturbative scale of the order $m_Q v^2$, which is not explicitly denoted because LDMEs is not evolved in practice but rather determined at the scale m_Q or $2m_Q$ as in conventional NRQCD approach.

[2]If one expresses the m_P in σ_0 in terms of m_Q and v^2, then one finds that

$$2m_P \left[1 + \langle v^2 \rangle c_{v^2}^{\mathrm{sing}} \right] = 4m_Q \sqrt{1 + \langle v^2 \rangle} \left[1 + \langle v^2 \rangle c_{v^2}^{\mathrm{sing}} \right] \approx \left[2\sqrt{m_Q} \left(1 - \frac{5}{12} \langle v^2 \rangle \right) \right]^2,$$

which agrees with $d_s^{(0)}$ and $d_s^{(v^2)}$ in eq. (2.26) of ref. [23].

where α is the fine structure constant, e_Q is the fractional charge of a heavy quark Q, m_P is the quarkonium mass, m_Q is the heavy quark mass, $\langle \mathcal{O}_1 \rangle_P = \langle 0|\chi^\dagger\psi|P\rangle\langle P|\psi^\dagger\chi|0\rangle$ is the non-relativistically normalized LO NRQCD LDME of the production of S-wave pseudoscalar quarkonium P, and the relativistic correction to the LO NRQCD LDME, $\langle v^2 \rangle$, is defined by

$$\langle v^2 \rangle \equiv \frac{1}{m_Q^2}\frac{\langle P|\psi^\dagger\left(-\frac{i}{2}\overleftrightarrow{\boldsymbol{D}}\right)^2\chi|0\rangle}{\langle P|\psi^\dagger\chi|0\rangle}, \tag{2.5}$$

where $\boldsymbol{D} = \boldsymbol{\nabla} - ig_s\boldsymbol{A}$ is the spartial part of the gauge-covariant derivative and $\psi^\dagger\overleftrightarrow{\boldsymbol{D}}\chi \equiv \psi^\dagger(\boldsymbol{D}\chi) - (\boldsymbol{D}\psi)^\dagger\chi$. $\tilde{e}_Q^2$ is given in eq. (2.19) which includes the effect of both of the virtual photon and Z boson propagators. To make our paper self-contained we also copy the fixed-order cross section in [17] into appendix A.

The nonsingular part is defined by subtracting the fixed-order singular part from the fixed-order cross section as

$$\sigma^{\mathrm{ns}}(r;\mu) = \sigma^{\mathrm{fixed}} - \sigma^{\mathrm{fixed\text{-}sing}} = -r\,\sigma_0\left[1 + \frac{\alpha_s C_F}{4\pi}c^{\mathrm{ns}} + \langle v^2 \rangle c_{v^2}^{\mathrm{ns}}\right], \tag{2.6}$$

where the coefficients are $c^{\mathrm{ns}} = (c^{\mathrm{fixed}} - c^{\mathrm{sing}})/(-r) \approx -14.9 - 4.8\log r + \log^2 r + O(r)$ and $c_{v^2}^{\mathrm{ns}} = (c_{v^2}^{\mathrm{fixed}} - c_{v^2}^{\mathrm{sing}})/(-r) = -1/3$. Note that we pull out a prefactor $-r$ in eq. (2.6) to imply the relative suppression of nonsingular part in small r region but this correction is still important at the Belle energy. The nonsingular part from the Z-boson contribution is about $4m_Q^2/m_Z^2$ and remains small near the resonance and we omit them in this paper.

Now the full cross section reproduces the ordinary fixed-order result when we turn off the RG evolution: $\sigma^{\mathrm{fixed}}(r;\mu) = \sigma(r;\mu,\mu,\mu)$. Therefore, at the energies where $\log r \sim O(1)$ hence $\mu \sim \mu_0$, the full cross section is consistent with the fixed-order results and at higher energies where $|\log r| \gg 1$ and $\mu \gg \mu_0$, the resummation implemented in full cross section becomes effective. Therefore the formula in eq. (2.1) gives correct results at wide range of energies of current and future colliders. For the precise predictions for various energies including current and future colliders, both of the resummation of large logarithms and the fixed-order computation should be improved equivalently.

Now let us discuss the amplitude for the singular part. In lepton collisions an initial lepton pair annihilates into virtual gauge bosons such as γ^* or, Z^*, then a pair of quark and anti-quark produced from the bosons turns into a bounded quarkonium state by emitting a photon. The scattering amplitude for a pseudoscalar quarkonium P plus a final photon can be written as

$$i\mathcal{M}(e^+e^- \to \gamma^*/Z^* \to P\gamma) = L_I^\mu\,\langle P(p) + \gamma(\epsilon,k)|J_V^\mu|0\rangle, \tag{2.7}$$

where the index $I = \gamma^*, Z^*$ represents the virtual bosons. The current has the vector and axial vector components: $J_V^\mu = \bar{\psi}\gamma^\mu\psi$ and $J_A^\mu = \bar{\psi}\gamma^\mu\gamma_5\psi$. But the axial current does not contribute due to the opposite charge conjugation and we only have J_V in eq. (2.7). The part L_I^μ contains a matrix element of initial lepton pair, a virtual boson propagator, and

electroweak charges of the quarks. Its expression is

$$
L_I^\mu = \begin{cases} \frac{ie_Q e^2}{s}\bar{v}(\bar{P})\gamma^\mu u(P), & \text{for } I = \gamma^*, \\[2mm] -\frac{ig_V^Q e^2/\sin^2(2\theta_W)}{s-m_Z^2}\bar{v}(\bar{P})\gamma^\mu(g_V^e - g_A^e\gamma_5)u(P), & \text{for } I = Z^*, \end{cases} \tag{2.8}
$$

where e is the electromagnetic coupling, e_Q is the fractional electric charge of the heavy quark Q, $\sqrt{s}$ is the CM collision energy, θ_W is the Weinberg angle, $g_V^e = -\frac{1}{2} + 2\sin^2\theta_W$ and $g_A^e = -\frac{1}{2}$ are the vector and axial charges of electron, and $g_V^Q = T_Q - 2e_Q\sin^2\theta_W$ with $T_Q = \pm 1/2$ is the vector charge of quark with a flavor $Q = c, b$, respectively.

The quark matrix element is extensively studied in the context of the meson form factor and the quark part in eq. (2.7) can be expressed in the form factor style as

$$
\langle P(p) + \gamma(\epsilon,k)|J_V^\mu|0\rangle = -i\epsilon_\nu^*(k)ee_Q\int d^4x e^{ik\cdot x}\left\langle P(p)\left|T\left[J_V^{\nu\dagger}(x)J_V^\mu(0)\right]\right|0\right\rangle
$$
$$
= i\epsilon_\nu^*(k)\,ee_Q\frac{\epsilon_\perp^{\mu\nu}}{2}\,G_P(\mu) + O(r)\,, \tag{2.9}
$$

where T is the time-ordered product and $\epsilon_\perp^{\mu\nu} = \epsilon^{\mu\nu\rho\sigma}p_\rho k_\sigma/(p\cdot k)$ is the asymmetric tensor.

2.1 Light-cone distribution amplitude

The factor $G_P(\mu)$ is the leading-twist result in LC factorization:

$$
G_P(\mu) \equiv f_P(\mu, m_Q)\int_0^1 dx\, T_H^P(x; \mu, \sqrt{s})\phi_P(x; \mu, m_Q), \tag{2.10}
$$

where T_H^P is the hard-scattering kernel, ϕ_P is the LCDA of a pseudoscalar quarkonium P, and f_P is the decay constant. The scale μ is an arbitrary energy scale that separates the natural scales m_Q and $\sqrt{s}$ which are the last arguments of each functions. Each function depends on the logarithm of their ratio: the natural scale to the scale μ. For simplicity, we omit the last arguments to the functions from now on.

The hard-scattering kernel $T_H^P(x; \mu)$ describes a production of quark and anti-quark pair at ${}^1S_0$ state. The one-loop expression is given in refs. [14, 33] by

$$
T_H^P(x,\mu) = T_H^{(0)}(x) + \frac{\alpha_s(\mu)}{4\pi}T_H^{(1)}(x,\mu) + O(\alpha_s^2), \tag{2.11}
$$

where

$$
T_H^{(0)}(x) = \frac{1}{\bar{x}} + (x \leftrightarrow \bar{x}), \tag{2.12a}
$$
$$
T_H^{(1)}(x,\mu) = \frac{C_F}{\bar{x}}\left[(3 + 2\log\bar{x})\left(\log\frac{s}{\mu^2} - i\pi\right) + \log^2\bar{x} + (8\Delta - 1)\frac{\bar{x}\log\bar{x}}{x} - 9\right]
$$
$$
+ (x \leftrightarrow \bar{x}), \tag{2.12b}
$$

here $\bar{x} \equiv 1-x$. Note that $\Delta = 0$ for the naive dimensional regularization (NDR) scheme [34] and $\Delta = 1$ for the t'Hooft-Veltman (HV) scheme [35, 36] for γ_5 regularization.[3] The scheme

---

[3]In the NDR scheme, $\{\gamma_5, \gamma^\mu\} = 0$, for the index μ in d dimension, while in the HV scheme, γ_5 defined in 4 dimension anticommutes $\{\gamma^\mu, \gamma_5\} = 0$ for $\mu = 0, 1, 2, 3$ but commutes $[\gamma^\mu, \gamma_5] = 0$ for $\mu = 4, \cdots, d$. Note that the δ in ref. [33] and the Δ in ref. [14] are related as $\delta = 1 - \Delta$.

dependence in the hard kernel is cancelled by the same term with the opposite sign in the LCDA.

The pseudoscalar LCDA is defined by a non-local matrix element of $\gamma^+\gamma_5$ as

$$\langle P(p)|\bar{Q}(z)\gamma^+\gamma_5[z,0]Q(0)|0\rangle = p^+ f_P \int_0^1 dx\, e^{ip\cdot zx}\phi_P(x,\mu)\,, \tag{2.13}$$

where the plus components are $\gamma^+ = \gamma^0 + \gamma^3$ and $p^+ = p^0 + p^3$. $x \in [0,1]$ is the collinear momentum fraction of a quark in the quarkonium and $[z,0]$ is the gauge link that is defined by

$$[z,0] = \mathcal{P}\exp\left[ig_s \int_0^z dy\, A_a^+ T^a\right]\,, \tag{2.14}$$

where $\mathcal{P}$ stands for path ordering, $g_s = \sqrt{4\pi\alpha_s}$ is the strong coupling constant, A^a is the gluon field with color index a, and T^a is fundamental representation of $\mathrm{SU}(N_c)$.

The LCDA ϕ_P describes the collinear-gluon exchange between quark and anti-quark pair and it is normalized to the unity upon the integration over x. This normalization defines the decay constant f_P to be eq. (2.13) at $z = 0$ and it describes a $c\bar{c}$ pair transition into a physical quarkonium.[4] In light mesons, the LCDA and the decay constant are non-perturbative and the former is modeled with a few parameters and the latter is determined by comparison to measurement. On the other hand in heavy quarkonium the LCDA and short-distance part of the decay constant are perturbatively calculable by matching QCD onto NRQCD amplitude. Their one-loop correction was obtained in [14] and the relativistic correction was obtained in [26, 37]. We treat v^2 and α_s corrections are of the same size and expand up to the same power. Then, the LCDA expanded up to the leading corrections in α_s and v^2 is

$$\phi_P(x,\mu) = \phi^{(0)}(x) + \frac{\alpha_s(\mu)}{4\pi}\phi^{(1)} + \langle v^2\rangle \phi^{(v^2)} + O(\alpha_s^2, \alpha_s v^2, v^4)\,, \tag{2.15}$$

where

$$\phi^{(0)} = \delta\left(x - \frac{1}{2}\right)\,,$$

$$\phi^{(1)} = C_F\theta(1-2x)$$
$$\times\left\{\left[4x\frac{\frac{1}{2}+\bar{x}}{\frac{1}{2}-x}\left(\log\frac{\mu_0^2}{4m_Q^2} - 2\log\left(\frac{1}{2}-x\right) - 1\right)\right]_+ + \left[\frac{4x\bar{x}}{(\frac{1}{2}-x)^2}\right]_{++} + \Delta\left[16x\right]_+\right\}$$
$$+ (x \leftrightarrow \bar{x})\,,$$

$$\phi^{(v^2)} = \frac{\delta^{(2)}(x-\frac{1}{2})}{24}\,, \tag{2.16}$$

and the $+$ and $++$ functions are defined in appendix B. The leading α_s and v^2 corrections to the decay constant f_P are given by

$$f_P(\mu) = \frac{\sqrt{2N_c}\sqrt{2m_P}\Psi_P(0)}{2m_Q}\left[1 - \langle v^2\rangle + \frac{\alpha_s(\mu)C_F}{4\pi}(-6 + 4\Delta) + O(\alpha_s^2, v^4, \alpha_s v^2)\right]\,, \tag{2.17}$$

---

[4]The definition of f_P is different from that of ref. [14] by a multiplicative factor i.

where $\Psi_P(0)$ is the wavefunction at the origin and is defined by $\Psi_P(0) = \langle P(p)|\psi^\dagger \chi|0\rangle/\sqrt{2N_c}$ and $|\Psi_P(0)|^2 = \langle \mathcal{O}_1 \rangle_P/(2N_c)$.[5] The relativistic correction agrees with the result in ref. [37] with $x_0 = \bar{x}_0 = 1/2$. The renormalon ambiguity coming from the pole mass can be avoided if we replace m_Q by $\overline{\text{MS}}$ mass.[6] Thus we replace the pole mass m_Q in eq. (2.17) with the one-loop corrected $\overline{\text{MS}}$ mass in ref. [39]: $m_Q = \overline{m}_Q [1 + \alpha_s(\overline{m}_Q)C_F/\pi]$ and truncate higher-order contributions than our working precisions. The singular part of the cross section can be written in terms of $G_P(\mu)$ in eq. (2.10) as

$$\sigma^{\text{sing}} = \frac{2\pi^2 e_Q^2 \tilde{e}_Q^2 \alpha^2(\sqrt{s})\alpha(0)}{3s^2}|G_P(\mu)|^2,\qquad(2.18)$$

where for the virtual photon $\tilde{e}_Q^2$ is e_Q^2, and for the virtual photon and Z boson it is

$$\tilde{e}_Q^2 = e_Q^2 - 2\frac{e_Q g_V^Q g_V^e}{\sin^2(2\theta_W)}\frac{1 - r_Z}{(1 - r_Z)^2 + r_Z\frac{\Gamma_Z^2}{s}} + \frac{(g_V^Q)^2[(g_V^e)^2 + (g_A^e)^2]}{\sin^4(2\theta_W)}\frac{1}{(1 - r_Z)^2 + r_Z\frac{\Gamma_Z^2}{s}},\quad(2.19)$$

where $r_Z = m_Z^2/s$. Note that eq. (2.18) is rather a fixed-order singular cross section in eq. (2.2) because the functions eqs. (2.11), (2.15) and (2.17) are in fixed-order form. We obtained the resummed singular part after the RG evolution and resummation, which is discussed next subsection.

We also give the expression for the decay rate of Z boson into a pseudoscalar quarkonium plus a photon in terms of $G_P(\mu)$ as

$$\Gamma^{\text{fixed-sing}}(r;\mu) = \frac{\pi\alpha(m_Z)\alpha(0)e_Q^2(g_V^Q)^2}{6m_Z \sin^2 2\theta_W}|G_P(\mu)|^2.\qquad(2.20)$$

2.2 RG equation and log resummation

The large logarithms in the cross section can be resummed by evolving each function in the factorization from its own natural scale, $\mu_0 \sim m_Q$ for the LCDA or $\mu \sim \sqrt{s}$ for the hard-scattering kernel T_H^P to a common scale $\tilde{\mu}$, which can be chosen to be an arbitrary scale between μ_0 and μ because the $\tilde{\mu}$ dependence should be exactly cancelled when evolutions of all the functions are combined together. One of the simple and conventional choices is to set $\tilde{\mu} = \mu$ then, the LCDA is just evolved from m_Q to μ, while the hard-scattering kernel is treated as fixed-order function.

The LCDA evolution is governed by the RG equation called the Efremov-Radyushkin-Brodsky-Lepage (ERBL) equation [9, 40]:

$$\mu^2\frac{\partial}{\partial\mu^2}[f_P(\mu)\phi_P(x,\mu)] = \int_0^1 dy\, V(x,y;\alpha_s(\mu))[f_P(\mu)\phi_P(y,\mu)],\qquad(2.21)$$

where the ERBL kernel $V(x,y;\alpha_s(\mu))$ for a pseudoscalar meson was extensively studied in the pion form factor. In the case of quarkonium the product $f_P\phi_P$ is factorized into

---

[5]We take the nonrelativistic normalization for the LDME while ref. [14] takes the relativistic normalization (see eq. (4.8)): $\langle O(^1S_0)\rangle = \sqrt{2m_P}\langle P(p)|\psi^\dagger\chi|0\rangle$.

[6]See, for example, ref. [38].

two parts LDME and short-distance coefficients as in eqs. (2.17) and (2.16) and the RG equation eq. (2.21) can be expressed into two set of RG equations: one for LDMEs and the other for the coefficients. The formal equation is evolved from LDME's natural scale $m_Q v^2$ to μ and the latter is from μ_0 to μ. This way would better fit to the philosophy of scale separation in effective field theory framework. However, LDME scale is nonperturbative and evolution from the scale would not work. Conventionally the LDMEs are determined at the scale μ_0 rather $m_Q v^2$. Then, we simply run both parts from μ_0 to μ by using eq. (2.21).

The LL and NLL accuracies are achieved by solving the ERBL equation with one- and two-loop kernels respectively. The kernel is known up to two loops in the NDR scheme and we use the NDR results to achieve NLL accuracy.

$$V(x,y;\alpha_s(\mu)) = \sum_{n=0}^{\infty} \left(\frac{\alpha_s(\mu)}{4\pi}\right)^{n+1} V^{(n)}(x,y)\,, \tag{2.22}$$

where the one-loop coefficient is given by

$$V^{(0)}(x,y) = 2C_F \left[\frac{1-x}{1-y}\left(1 + \frac{1}{x-y}\right)\theta(x-y) + \frac{x}{y}\left(1 + \frac{1}{y-x}\right)\theta(y-x)\right]_+\,, \tag{2.23}$$

and the two-loop expression can be found in refs. [41–44]. The eigenfunction of the one-loop kernel $V^{(0)}(x,y)$ is G_n whose eigenvalue is $-\gamma_n^{(0)}/2$:

$$\int_0^1 dy\, V^{(0)}(x,y)G_n(y) = -\frac{\gamma_n^{(0)}}{2}\, G_n(x), \tag{2.24}$$

where G_n is the product of the Gegenbauer polynomial $C_n^{(3/2)}$ and its weight [45]:

$$G_n(x) = x(1-x)C_n^{(3/2)}(2x-1). \tag{2.25}$$

$\gamma_n^{(0)}$ is the LO anomalous dimension and here we follow the convention of ref. [46]

$$\gamma_n^{(0)} = 8C_F \left[H_{n+1} - \frac{1}{2(n+1)(n+2)} - \frac{3}{4}\right]. \tag{2.26}$$

The NLO anomalous dimension $\gamma_n^{(1)}$ is defined in the same way from the 2-loop kernel $V^{(1)}(x,y)$. The solution of the ERBL equation is expressed as a series sum,

$$\phi_n(\mu) = \sum_{k=0}^{n} U_{nk}(\mu,\mu_0)\phi_k(\mu_0)\,, \tag{2.27}$$

where the k-th Gegenbauer coefficient of LCDA at the scale μ_0 is

$$\phi_n(\mu_0) = N_n \int_0^1 dx\, \phi_P(x,\mu_0)C_n^{(3/2)}(2x-1)\,, \tag{2.28}$$

with $N_n = 4(2n+3)/[(n+1)(n+2)]$. The coefficient at LO is simple

$$\phi_n^{(0)} = N_n C_n^{(3/2)}(0)\,, \tag{2.29}$$

where $C_n^{(3/2)}(0) = (-1)^{n/2} \frac{(n+1)!!}{n!!}$ for even n and zero for odd n. Explicitly, the LO ERBL equation for the n-th moment of the LCDA is given by

$$\mu^2 \frac{d}{d\mu^2} [f_P(\mu)\phi_n(\mu)] = \frac{\alpha_s(\mu)}{4\pi} \frac{(-\gamma_n^{(0)})}{2} [f_P(\mu)\phi_n(\mu)]. \tag{2.30}$$

Following the convention of ref. [46], the solutions of the scale evolution factor $U_{nk}(\mu, \mu_0)$ up to NLL accuracy are given by

$$U_{nk}(\mu, \mu_0) = \left[\frac{\alpha_s(\mu)}{\alpha_s(\mu_0)} \right]^{\frac{\gamma_n^{(0)}}{2\beta_0}} \tag{2.31}$$
$$\times \left[\delta_{nk} \left(1 + \frac{\alpha_s(\mu) - \alpha_s(\mu_0)}{4\pi} \frac{\gamma_n^{(1)}\beta_0 - \gamma_n^{(0)}\beta_1}{2\beta_0^2} \right) + (1 - \delta_{nk})d_{nk}(\mu, \mu_0)\frac{\alpha_s(\mu)}{4\pi} \right],$$

where the value of U_{nk} at LL accuracy is nonzero only for $n = k$: $[\alpha_s(\mu)/\alpha_s(\mu_0)]^{\gamma_n^{(0)}/(2\beta_0)} \delta_{nk}$. At NLL it is nonzero when $(n - k)$ is zero or, even and positive integer. β_n is the beta function coefficients for $(n + 1)$-th order in α_s and the explicit expressions of the two-loop anomalous dimensions $\gamma_n^{(1)}$ and d_{nk} are copied in appendix C.

Then, the RG evolved function $G_P(\mu)$ is given by

$$G_P(\mu) = f_P \left\{ \mathcal{M}^{(0,0)}(\mu) + \frac{\alpha_s(\mu)}{4\pi} \mathcal{M}^{(1,0)}(\mu) + \langle v^2 \rangle_P \mathcal{M}^{(0,v^2)}(\mu) + \frac{\alpha_s(\mu_0)}{4\pi} \mathcal{M}^{(0,1)}(\mu) \right\}, \tag{2.32}$$

where $\mathcal{M}^{(i,j)}$ are defined in terms of the RG evolved LCDA in eq. (2.27)

$$\mathcal{M}^{(i,j)}(\mu) = \sum_{n=0}^{\infty} T_n^{(i)}(\mu)\phi_n^{(j)}(\mu), \tag{2.33}$$

and

$$T_n^{(i)}(\mu) = \int_0^1 dx \, T_H^{(i)}(x, \mu) G_n(x) \tag{2.34}$$

is the coefficient in the expansion with Gegenbauer polynomials and it is non-vanishing only for even n because T_H^P is symmetric with respect to $x = 1/2$ while $G_n(x)$ is asymmetric for odd n. The LO coefficient for even n is simple

$$T_n^{(0)} = 1. \tag{2.35}$$

We would like to note that the decay constant f_P in eq. (2.32) is not evolved at NLL because its one- and two-loop anomalous dimensions in eqs. (2.26) and (C.1) are zeros: $\gamma_0^{(0)} = \gamma_0^{(1)} = 0$. One can see this explicitly by taking the 0-th Gegenbauer coefficient of ϕ_P in eq. (2.21), or in eq. (2.30) because $\phi_0(\mu) = 1$ for all μ. We also emphasize that the relativistic correction $\mathcal{M}^{(0,v^2)}(\mu)$ correctly resums logarithms proportional to $\langle v^2 \rangle \alpha_s^n \log^n r$ by using the same RG evolution U_{nk} and its expansion in α_s is given by

$$G_P \propto \langle v^2 \rangle \left[-\frac{5}{3} + \frac{27 - 10\log 2}{3} \frac{\alpha_s(\mu_0^2)C_F}{4\pi} \log \frac{\mu_0^2}{\mu^2} \right]. \tag{2.36}$$

This agrees with the logarithmic term in $\alpha_s\langle v^2 \rangle$ correction eq. (2.26) in [23].

Eventually we insert eq. (2.32) into eq. (2.18) and obtain the singular part and full cross section in eq. (2.1). In practice of computation there is an option of truncating higher-order terms irrelevant at our NLL accuracy and we make following truncations. In eq. (2.32), the first term $\mathcal{M}^{(0,0)}$ is computed using NLL expression of U_{nk} while the other $\mathcal{M}^{(i,j)}$ terms are computed using LL expression. In the absolute square $|G_P(\mu)|^2$, we also drop higher-order terms proportional to α_s^2 or $\alpha_s \langle v^2 \rangle$, which are obtained in the product of $\mathcal{M}^{(i,j)}$ in eq. (2.32) and f_P in eq. (2.17).

We also adopt the Abel-Padé method developed and used in [27–29] to achieve faster numerical convergence at NLL accuracy and to deal with divergences associated with the relativistic corrections in LCDA.

2.3 γ_5-scheme dependence

As we can see from eqs. (2.12b), (2.16) and (2.17), there are γ_5 scheme dependences in the hard kernel $T_H(x, \mu)$, LCDA $\phi_P(x, \mu)$ and decay constant $f_P(\mu)$, which are represented by the terms proportional $\Delta = 0, 1$ for NDR and HV schemes, respectively. It is easy to check that the Δ dependences of the factor $G_P(\mu)$ vanish at NLO without resummation or, RG evolution. However, it is not obvious whether the Δ dependences vanish or not at NLL accuracy due to additional scheme dependence that may enter in two-loop anomalous dimension $\gamma_n^{(1)}$. Note that $\gamma_n^{(0)}$ is Δ-independent and so is the LL resummation. ref. [47] computed the n_f-dependent part of two-loop evolution kernel $V^{(1)}(x, y)$ in both NDR and HV schemes and we can obtain the scheme dependence for full two-loop evolution kernel by combining eqs. (5.24), (5.35), and (5.41a) and applying the relation in eq. (5.40) in ref. [47], which gives

$$\Delta V^{(1)}(x, y) = -8\Delta C_F \beta_0 \left[\frac{x}{y}\theta(y - x) + \frac{1 - x}{1 - y}\theta(x - y) \right].$$ (2.37)

Again, polynomials $G_n(x)$ is the eigenfunction of $\Delta V^{(1)}$ with the eigenvalue anomalous dimension

$$\int_0^1 dy \ \Delta V^{(1)}(x, y)G_n(y) = -\frac{\Delta \gamma_n^{(1)}}{2}G_n(x) \,,$$ (2.38)

where analytic expression of the anomalous dimension is given by

$$\Delta \gamma_n^{(1)} = \Delta \frac{16 C_F \beta_0}{(n + 1)(n + 2)} \,.$$ (2.39)

At NLL, there are two types of Δ dependences in the amplitude $G_P(\mu)$. The one from NLL evolution factor U_{nk} in eq. (2.31) is proportional to the anomalous dimension in eq. (2.39):

$$\Delta_n^{(a)} = G_{P,n}^{\mathrm{LL}}(\mu)\frac{\alpha_s(\mu) - \alpha_s(\mu_0)}{4\pi}\frac{\Delta \gamma_n^{(1)}}{2\beta_0} \,.$$ (2.40)

Here $G_{P,n}^{\mathrm{LL}}(\mu) = \left[\frac{\alpha_s(\mu)}{\alpha_s(\mu_0)} \right]^{\frac{\gamma_n^{(0)}}{2\beta_0}} f_P^{(0)} T_n^{(0)} \phi_n^{(0)}$ is the LL amplitude, where $f_P^{(0)} = \sqrt{N_c m_P}\Psi_P(0)/m_Q$ is LO decay constant and $T_n^{(0)}$, $\phi_n^{(0)}$ are given in eqs. (2.29) and (2.35).

The other type of Δ dependence is those from one-loop corrections $f_P^{(1)}, T_n^{(1)}, \phi_n^{(1)}$. The terms proportional to Δ are given by non-logarithmic constant parts

$$\Delta f_P^{(1)} = 4C_F f_P^{(0)} \Delta, \tag{2.41}$$

$$\Delta T_n^{(1)} = 8C_F \Delta \int_0^1 dx \frac{1}{x\bar{x}}(x \ln x + \bar{x} \ln \bar{x}) G_n(x), \tag{2.42}$$

$$\Delta \phi_n^{(1)} = 16C_F \Delta N_n \int_0^1 dx \big[\theta(1-2x)[x]_+ + \theta(1-2\bar{x})[\bar{x}]_+\big] C_n^{(3/2)}(2x-1). \tag{2.43}$$

Collecting three contributions above, we have

$$\begin{aligned}\Delta_n^{(b)} &= G_{P,n}^{\mathrm{LL}}(\mu)\bigg(\frac{\alpha_s(\mu_0)}{4\pi}\Delta f_P^{(1)}/f_P^{(0)} + \frac{\alpha_s(\mu_0)}{4\pi}\Delta\phi_n^{(1)}/\phi_n^{(0)} + \frac{\alpha_s(\mu)}{4\pi}\Delta T_n^{(1)}/T_n^{(0)}\bigg) \\ &= G_{P,n}^{\mathrm{LL}}(\mu)\bigg(\frac{\alpha_s(\mu)}{4\pi}\Big[\Delta f_P^{(1)}/f_P^{(0)} + \Delta\phi_n^{(1)}/\phi_n^{(0)} + \Delta T_n^{(1)}/T_n^{(0)}\Big] \\ &\quad + \frac{\alpha_s(\mu_0) - \alpha_s(\mu)}{4\pi}\Big[\Delta f_P^{(1)}/f_P^{(0)} + \Delta\phi_n^{(1)}/\phi_n^{(0)}\Big]\bigg). \end{aligned} \tag{2.44}$$

In the second equality we rearranged terms into two parts, the one proportional to NLO correction evaluated at the α_s scale μ and the other proportional to the difference $\alpha_s(\mu_0) - \alpha_s(\mu)$ which is a part of NLL resummation. The scheme independence at fixed-order NLO implies the cancellation of first part

$$\Delta f_P^{(1)}/f_P^{(0)} + \Delta\phi_n^{(1)}/\phi_n^{(0)} + \Delta T_n^{(1)}/T_n^{(0)} = 0. \tag{2.45}$$

This is also confirmed by explicit computing $\Delta T_n^{(1)}$ and $\Delta\phi_n^{(1)}$ which are zero for odd n and

$$\Delta T_n^{(1)} = -\frac{8C_F\Delta}{(n+1)(n+2)}, \tag{2.46}$$

$$\Delta\phi_n^{(1)} = -4C_F\Delta N_n C_n^{(3/2)}(0)\left(1 - \frac{2}{(n+1)(n+2)}\right), \tag{2.47}$$

for even n. We would like to note an interesting relation between $\Delta T_n^{(1)}$ and $\Delta\gamma_n^{(1)}$:

$$\Delta T_n^{(1)} = -\Delta\gamma_n^{(1)}/(2\beta_0) \tag{2.48}$$

or, $\Delta\phi_n^{(1)}/\phi_n^{(0)} + \Delta f_P^{(1)}/f_P^{(0)} = \Delta\gamma_n^{(1)}/(2\beta_0)$ equivalently. This implies that the constant term in the one-loop functions completely determines Δ dependence of two-loop evolution kernel and this ensures the cancellation of $\Delta_n^{(a)}$ and $\Delta_n^{(b)}$:

$$\Delta_n^{(a)} + \Delta_n^{(b)} = G_{P,n}^{\mathrm{LL}}(\mu)\frac{\alpha_s(\mu) - \alpha_s(\mu_0)}{4\pi}\left[\frac{\Delta\gamma_n^{(1)}}{2\beta_0} + \Delta T_n^{(1)}/T_n^{(0)}\right] = 0, \tag{2.49}$$

where in $\Delta_n^{(b)}$ we eliminated $\Delta f_n^{(1)}$ and $\Delta\phi_n^{(1)}$ in favor of $\Delta T_n^{(1)}$ by using eq. (2.45). Therefore, γ_5 scheme independence is valid at NLL accuracy.

At higher-order, we expect a similar pattern of cancellation between Δ dependent terms: cancellation between fixed-order terms at the same α_s scale as in eq. (2.45) and cancellations between n-loop anomalous dimension from evolution factor and the constant terms of $(n-1)$-loop function as in eq. (2.49).

2.4 Logarithmic structure

Here we discuss logarithmic structure and accuracy of the resummed amplitude. Even though this section explains quite well-known properties of resummation and does not contain anything new, it may be useful for those who are not familiar with resummation.

Let us first look at the fixed-order expansion of amplitude in eq. (2.10). Its logarithmic structure can be schematically expressed as

$$
\begin{aligned}
G_P^{\text{fixed}} = c_{00} \ &+ \frac{\alpha_s}{4\pi}(c_{11}L + c_{10}) \\
&+ \left(\frac{\alpha_s}{4\pi}\right)^2 (c_{22}L^2 + c_{21}L + c_{20}) + \cdots,
\end{aligned}
\tag{2.50}
$$

where $L \equiv \log(4m_Q^2/s)$. The largest logarithmic term at each α_s order is $\alpha_s^n L^n$ and then the next largest is $\alpha_s^n L^{n-1}$. The functions T_H and ϕ are first expanded with the Gegenbauer polynomials, then each coefficient is resummed as $G_P^{nk} = f_P T_n U_{nk} \phi_k$, and summation over all n and k gives the resummed G_P. The individual G_P^{nk} takes the following form

$$
\begin{aligned}
G_P^{nk} = C(\alpha_s) \ \exp \Bigg[\ &\frac{\alpha_s}{4\pi}(C_{11}L + C_{10}) \\
&+ \left(\frac{\alpha_s}{4\pi}\right)^2 (C_{22}L^2 + C_{21}L + C_{20}) + \cdots \Bigg] \\
&\quad\text{LL} \quad + \text{NLL} \ + \cdots,
\end{aligned}
\tag{2.51}
$$

where $C(\alpha_s)$ is the fixed-order expansion in α_s and it does not depend on the logarithms,

$$
C(\alpha_s) = C_0 + \frac{\alpha_s}{4\pi}C_1 + \cdots.
\tag{2.52}
$$

The fixed-order coefficient C_i is given by fixed-order function T_n, ϕ_k, f_P and the coefficients C_{ij} associated with anomalous dimensions are given by U_{nk} in eq. (2.31). Therefore, in general the coefficients C_i and C_{ij} differ for the different values of n, k. For example, C_0 is non-zero for the diagonal element where $n = k$ but zero otherwise. We are implicit with those n, k dependence to make our discussion focused on the logarithmic structure. Similarly, we do not separately discuss about v^2 corrections in the coefficients C_i and it follows the same conclusion.

In the fixed-order perturbation theory, the series in eq. (2.50) are summed row-by-row, i.e., order-by-order in α_s. On the other hand, in resummed perturbation theory, the series in the exponent of eq. (2.51) are summed column-by-column, based on large-logarithmic power counting $L \sim 1/\alpha_s$. In eq. (2.51), the first column is of the order $\alpha_s^n L^n \sim 1$ called the LL, the second column is $\alpha_s^n L^{n-1} \sim \alpha_s$ called the NLL, and so on. It is clear that which fixed-order terms in eq. (2.52) should be included: C_0 at LL and C_1 at NLL.

However, one may realize that the structure of evolution factor U_{nk} in eq. (2.31) is different from that of eq. (2.51). For example, the non-exponent term contains logarithms: $\alpha_s(\mu) - \alpha_s(\mu_0) = -\frac{\alpha_s(\mu_0)^2}{2\pi}\beta_0 \log(\mu/\mu_0) + \cdots$. This is because, in eq. (2.51) the second column is of $O(\alpha_s)$ hence those terms beyond LL can be expanded and moved down from

the exponent:

$$G_P^{nk} = C(\alpha_s) \left(1 + \frac{\alpha_s}{4\pi} C_{10} + \left(\frac{\alpha_s}{4\pi}\right)^2 C_{21} L + \cdots \right) \exp\left[\frac{\alpha_s}{4\pi} C_{11} + \left(\frac{\alpha_s}{4\pi}\right)^2 C_{22} L^2 + \cdots \right]$$

$$= \tilde{C}(\alpha_s) \exp\left[\frac{\alpha_s}{4\pi} C_{11} + \left(\frac{\alpha_s}{4\pi}\right)^2 C_{22} L^2 + \cdots \right], \qquad (2.53)$$

where $\tilde{C}(\alpha_s)$ includes two prefactors

$$\tilde{C}(\alpha_s) = C_0 + \frac{\alpha_s}{4\pi}\left[C_1 + C_0 \sum_{n=0} C_{1n} \left(\frac{\alpha_s L}{4\pi}\right)^n \right] + \cdots . \qquad (2.54)$$

We have LL accuracy with first term in eq. (2.54) and NLL with $O(\alpha_s)$ terms in the large-logarithmic power counting $\alpha_s^{n+1} L^n \sim \alpha_s$. This alternative way of arranging logarithms is equivalent to eq. (2.51) up to higher-order corrections than working accuracy and is the formula we use in this paper.

3 Numerical results

In this section, we list input parameters for numerical calculations then, present our results for the final state $\eta_{c,b} + \gamma$ in e^+e^- collisions at various collision energies and in Z-boson decay. Those results include the resummation at NLL accuracy, the fixed-order correction at NLO, and the relativistic corrections of the order v^2 as we discussed in previous sections. The numerical results at LL and NLL+NLO are compared and their perturbative convergence is discussed.

3.1 Input parameters and NRQCD matrix elements

We use PDG values for $\overline{\text{MS}}$ mass $\overline{m}_c = 1.275^{+0.025}_{-0.035}$ GeV and $\overline{m}_b = 4.18^{+0.04}_{-0.03}$ GeV, which gives the one-loop pole mass $m_c = 1.483^{+0.029}_{-0.041}$ GeV and $m_b = 4.58^{+0.04}_{-0.03}$ GeV and for Z-boson mass and width $m_Z = 91.1876 \pm 0.0021$ GeV and $\Gamma_Z = 2.4952 \pm 0.0023$ GeV. We run the coupling constants for the electroweak using the code Global Analysis of Particle Properties (GAPP) [48, 49] and the coupling constants for the strong interaction using the 4-loop expression of the QCD beta function [50]. The CM energies of B-, Z- and Higgs factories are $\sqrt{s} = 10.58, 91.19, 240$ GeV and the values of coupling at respective energies are $\alpha^{-1}(\sqrt{s}) = 130.855, 127.916, 127.473$, $\sin\theta_W(\sqrt{s}) = 0.233543, 0.231201, 0.236168$, and $\alpha_s(\sqrt{s}) = 0.1768, 0.1184, 0.1033$.

The NRQCD matrix elements such as the wave function at the origin and relative velocity were determined in [51] by using two constraints: electromagnetic decay rate $\Gamma[\eta_c \to \gamma\gamma]$ of order α_s and the potential model. These values need updates due to changes in input parameters: charm-quark pole mass, scale of α_s from $m_{\eta_c}/2$ to $2\overline{m}_c$, experimental value of the decay rate. In the determinations of $\langle\mathcal{O}_1\rangle_{\eta_c}$ and $\langle v^2\rangle_{\eta_c}$, we used the same string tension $\sigma = 0.1682 \pm 0.0053$ GeV^2 [51] and updated values for the 1-loop pole mass $m_c = 1.483^{+0.029}_{-0.041}$ GeV, the mass difference between J/ψ and $\psi(2S)$ $m_{2S} - m_{1S} = 589.188 \pm 0.028$ MeV, and the decay rate $\Gamma[\eta_c \to \gamma\gamma] = 5.0 \pm 0.4$ keV.[7] Differently from [51],

---

[7]This is 30% smaller than the value $7.2 \pm 0.7 \pm 2.0$ keV used in [51].

we do not take average with $\langle\mathcal{O}_1\rangle_{J/\psi}$ in the determination of $\langle\mathcal{O}_1\rangle_{\eta_c}$. In the decay rate formula, we have set the scale $\mu = 2\overline{m}_c$. The updated values are as follow:

$$\langle\mathcal{O}_1\rangle_{\eta_c} = 0.302^{+0.052}_{-0.049} \text{ GeV}^3, \tag{3.1}$$

$$\langle v^2\rangle_{\eta_c} = 0.222^{+0.070}_{-0.070}. \tag{3.2}$$

The uncertainty includes variations of σ, m_c, $m_{2S} - m_{1S}$, $\Gamma[\eta_c \to \gamma\gamma]$. And we assumed the size of the neglected higher-order corrections in α_s and v^2 to be 30% times the central values of α_s and v^2, respectively. Major sources of uncertainty are the variation of σ and the assumed higher-order corrections.

We like to pay a bit more attention to using those values in eq. (3.1). In conventional predictions, we may use the same value for the predictions at LO, NLO, and higher-order accuracy. This way can correctly reproduce the input decay rate using its 1-loop expression, while with LO expression of the decay rate the result is systematically biased by the amount of 1-loop correction included in the matrix element. Of course it is not a problem when the size of 1-loop correction is small as in bottomonium. However in the case of η_c we find the effect is as large as 40% due to large coupling constant $\alpha_s(2\overline{m}_c) \sim 0.27$. A similar bias exists in the cross sections and leads to overshooting in its predictions at LO. Eventually it would spoil the perturbative convergence due to a large change from LO to NLO and similarly from LL to NLL.

We can avoid this systematic bias once we use the matrix element determined at the same order with working order, at which we make predictions. By doing this the (experimental) input decay rate is always reproduced at each order in α_s. This can be done by replacing the NRQCD matrix element with the experimental value of decay rate multiplied by short distance coefficient:

$$\langle\mathcal{O}_1\rangle_{\eta_Q} = \Gamma_{\exp}\frac{m_Q^2}{2\pi\alpha^2(0)e_Q^4}\left[1 + \frac{4}{3}\langle v^2\rangle + \frac{\alpha_s(\mu)C_F}{\pi}\frac{20-\pi^2}{4}\right], \tag{3.3}$$

where the experimental value for η_c is $\Gamma_{\exp} = 5.0 \pm 0.4\,\text{keV}$ [52]. We insert eq. (3.3) into eq. (2.17) and truncate higher-order terms than the working order. One of advantages using eq. (3.3) is that the error propagations associated with the pole mass and the NRQCD matrix element $\langle\mathcal{O}_1\rangle_{\eta_c}$ become simpler. The pole mass m_Q^2 are cancelled by that of eq. (2.4) in the cross section. The perturbative uncertainty obtained from scale variation of eq. (3.3) largely contributes to uncertainty of $\langle\mathcal{O}_1\rangle_{\eta_c}$ and this contribution is now naturally combined in a correlated way with scale variations of the other part in the cross section. Another advantage from an empirical observation is that the 1-loop correction in the decay constant reduces significantly due to the large cancellation between $O(\alpha_s)$ terms of the decay constant eq. (2.17) and the decay rate in eq. (3.3) as

$$\begin{aligned}|f_{\eta_Q}(\mu)|^2 &= \frac{2m_P\langle\mathcal{O}_1\rangle_{\eta_Q}}{4m_Q^2}\left[1 - 2\langle v^2\rangle + \frac{\alpha_s(\mu)C_F}{\pi}(-3)\right] \\ &= \Gamma_{\exp}[\eta_Q \to \gamma\gamma]\frac{m_P}{4\pi\alpha^2(0)e_Q^4}\left[1 + \frac{\alpha_s(\mu)C_F}{\pi}\frac{8-\pi^2}{4} - \frac{2}{3}\langle v^2\rangle\right].\end{aligned} \tag{3.4}$$
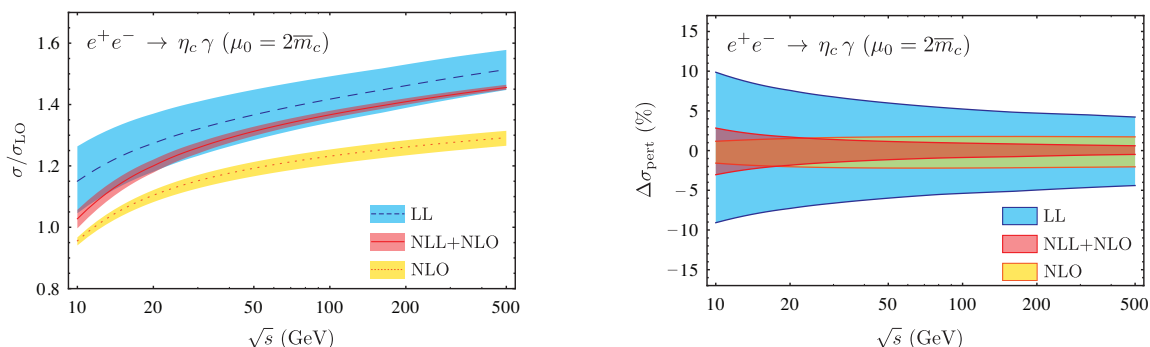
Figure 1. Left panel: LL, NLL+NLO and NLO cross sections normalized by the LO cross section. The scale choices are $\mu_0 = 2\overline{m}_c$ and $\mu = \sqrt{s}$. Bands are perturbative uncertainties only. right panel: perturbative uncertainties in percentage.
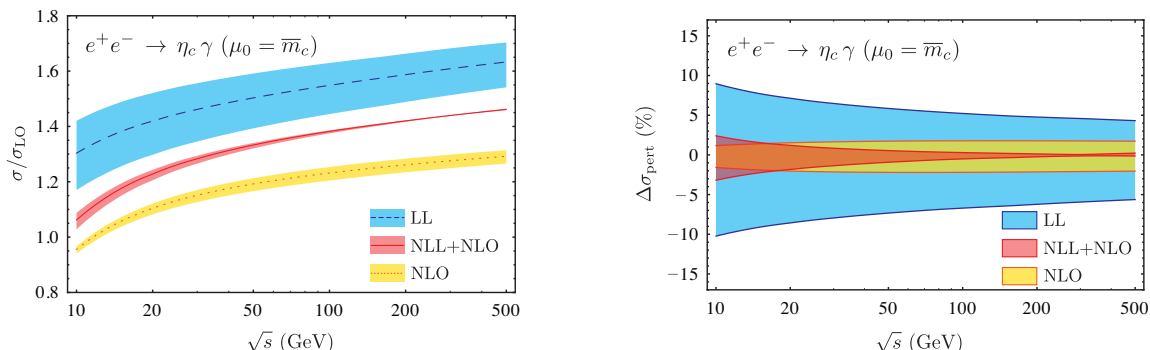

Figure 2. The same results with figure 1 except for $\mu_0 = \overline{m}_c$.

Note that the coefficient of $\alpha_s C_F/\pi$ reduces from -3 to $(8-\pi^2)/4 \approx -0.5$ and the coefficient of $\langle v^2 \rangle$ changes from -2 to $-2/3$. In this way, we have better perturbative convergence between LL and NLL (LO and NLO).

3.2 Final results

Our numerical results for $\eta_c + \gamma$ cross sections and perturbative uncertainties at different accuracies are given in figure 1. Three accuracies LL, NLL combined with NLO non-singular part and leading v^2 correction (NLL+NLO), fixed-order NLO are compared. The bands on left and right panels are absolute and relative perturbative uncertainties. The cross section in figures is scaled by the LO cross section

$$\sigma_{\mathrm{LO}} = \frac{8\pi\alpha^2(\sqrt{s})\tilde{e}_Q^2 m_P}{3\alpha(0)e_Q^2 s^2}\Gamma_{\mathrm{exp}}\,. \tag{3.5}$$

The values of scales we choose for LL and NLL+NLO are $\mu_0 = 2\overline{m}_c$ and $\mu = \mu_{\mathrm{ns}} = \sqrt{s}$ and for NLO we set all scales to be the same $\mu_0 = \mu = \mu_{\mathrm{ns}} = \sqrt{s}$. The perturbative uncertainties are estimated by varying μ, μ_{ns} from its central value by a factor 2 up and down and by varying μ_0 by a factor of $\sqrt{2}$. The uncertainties are summed in quadratures as in [31]:
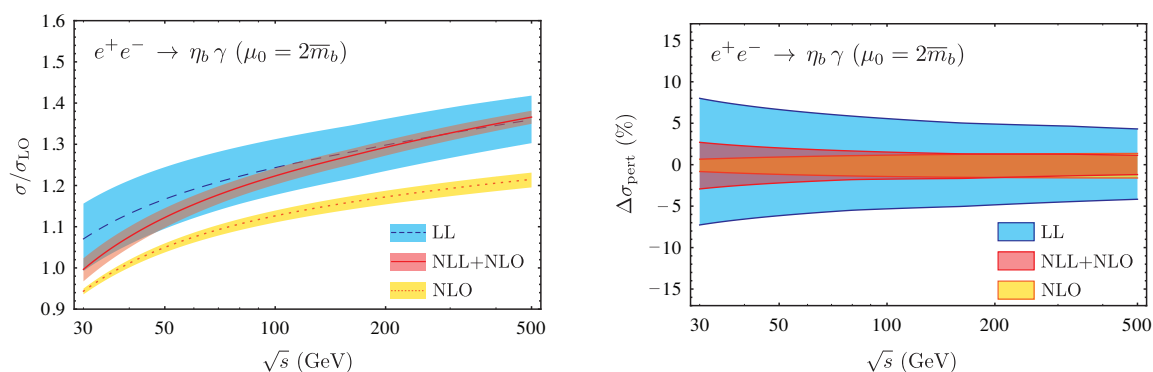
Figure 3. Left panel: LL, NLL+NLO and NLO cross sections normalized by LO cross section with $\mu_0 = 2\overline{m}_b$. right panel: corresponding perturbative uncertainties in percentage.

$\sqrt{\delta\sigma_{\mu_0}^2 + \delta\sigma_\mu^2 + \delta\sigma_{\mu_{ns}}^2}$, where $\delta\sigma_{\mu_i}$ is the change of cross section by a scale variation of μ_i. Here we do not include other sources of uncertainty to show the perturbative convergence and they will be included later in the final results in table 1. The perturbative uncertainty (width of the band) decreases by a factor of α_s from LL to NLL+NLO and a reasonable overlapping between two bands in left panel implies a good perturbative convergence. With increasing CM energy, the deviation of NLO from NLL+NLO becomes more significant due to the large logarithms not taken into account at NLO and this clearly shows that the small perturbative uncertainty of NLO is not reliable at this high energies.

In figure 2 we also show the results with a smaller value of μ_0: $\mu_0 = \overline{m}_c$ instead of $2\overline{m}_c$. The NLL perturbative uncertainty at $\mu_0 = \overline{m}_c$ tends to be asymmetric and smaller than that for $\mu_0 = 2\overline{m}_c$ because the lower scale variation from $\overline{m}_c$ by a factor of $\sqrt{2}$ moves μ_0 close to the Landau pole and the scale dependence near this region is not monotonic. In comparison to figure 1 at $\mu_0 = 2\overline{m}_c$ we observe relatively better perturbative convergence between LL and NLL although the other is still reasonable. For these reasons we take $\mu_0 = 2\overline{m}_c$ for our final results listed in table 1.

In figure 3 we also show the bottomonium production cross sections and their percent perturbative uncertainties, which are smaller compared those for charmonium. The decay rate for η_b is not available we use following value $\Gamma[\eta_b \to \gamma\gamma] = 0.512^{+0.096}_{-0.094}$ keV and for relative velocity $\langle v^2 \rangle_{\eta_b} = -0.009^{+0.003}_{-0.003}$ taken from [53].[8] The central values of scales are $\mu_0 = 2\overline{m}_b$ and $\mu = \mu_{ns} = \sqrt{s}$ and their variations are done in same way as for the charmonium.

Table 1 lists our final results for the cross sections at B-, Z- and Higgs-factory energies: $\sqrt{s} = 10.58$, 91.2, and $240\,\text{GeV}$ and Z-boson decay branching fractions. The uncertainties in the table for charmonium (η_c) channel includes uncertainties of input decay rate Γ^{exp} ($\pm 8\%$), relative velocity $\langle v^2 \rangle$ ($\pm 30\%$) as well as perturbative uncertainties ($\pm 3\%$ or less)

---

[8]Note that there is no restriction to the positive definiteness of the matrix element $\langle v^2 \rangle$. The matrix element $\langle v^2 \rangle$ intrinsically contains a linear ultraviolet (UV) divergence that must be regulated. For example, if we employ dimensional regularization that is consistent with existing calulations of quarkonum decay and production rates at relative order α_s and α_s^2, then the scaless power divergent integrals are discarded. Such subtractions of divergent contributions can lead to both positive and negative values. See ref. [54] for more details.

$\sqrt{s}$	Cross section		Branching fraction	
	η_c	η_b	η_c	η_b
$10.58\,\mathrm{GeV}$	$32.7 \pm 2.8\,\mathrm{fb}$	—		
m_Z	$0.449 \pm 0.037\,\mathrm{fb}$	$1.66 \pm 0.31\,\mathrm{fb}$	$(7.42 \pm 0.61) \times 10^{-9}$	$(2.80 \pm 0.53) \times 10^{-8}$
$240\,\mathrm{GeV}$	$0.189 \pm 0.016\,\mathrm{ab}$	$0.0934 \pm 0.0176\,\mathrm{ab}$		

Table 1. Cross sections $\sigma(e^+e^- \to \eta_Q + \gamma)$ and branching fractions $\mathrm{Br}(Z \to \eta_Q + \gamma)$ for charmonium and for bottomonium with uncertainties including all input parameters as well as perturbative uncertainties.

shown figure 1 and they are added in quadratures. For the bottomonium (η_b) the uncertainties are input decay rate ($\pm 20\%$), relative velocity ($\pm 30\%$), perturbation ($\pm 3\%$ or less). The final uncertainties quoted in table 1 are dominated by uncertainty of input decay rate.[9]

There is an independent prediction for $\langle v^2 \rangle_{\eta_b} = 0.042$ in ref. [55]. The authors of that reference have determined that value by making use of the Gremm-Kapustin relation. If we use this numerical value to compute the branching fraction for $e^+e^- \to \eta_b + \gamma$ at $\sqrt{s} = m_Z$ given in table 1, we obtain 2.78×10^{-8}, which is well within the prediction $(2.80 \pm 0.53) \times 10^{-8}$ given in table 1. However, we have not included the corresponding analysis into our final results listed in table 1 because the determination of $\langle v^2 \rangle$ by making use of either the lattice or Gremm-Kapustin approaches suffers too large uncertainties to determine even the signs of the matrix elements as is stated in ref. [54].

4 Comparison to various predictions and Belle's upper limit

In figure 4, we summarize the status of NRQCD predictions (points) in comparison with Belle's upper limit (90% credibility level) [30] (gray line) for $\sigma(e^+e^- \to \eta_c + \gamma)$ at $\sqrt{s} = 10.58\,\mathrm{GeV}$. Since the resummation effect is not substantial at this energy our results LL and NLL+NLO+v^2 on the right side of the plot should be comparable to LO and to NLO with v^2 corrections.

For a fair comparison with previous predictions we need to point out several major differences of input parameters and their variations between different predictions. First, a small error bar of NLO [19] and invisibly small error of NNLO [21] only include a charm-quark mass variation by $0.1\,\mathrm{GeV}$ and they should not be compared to full uncertainties of other predictions. Instead their central values can be compared with the others. Second, LO, NLO+v^2 [17], and NLO+v^2 resummation [22] use the LDME of [51], which should be updated with improved measurement of $\Gamma[\eta_c \to \gamma\gamma]$ as discussed around eq. (3.1) and with the updated LDME, we expect decrease of the cross section by about $10 \sim 20\%$ and also reduction of their uncertainties, quantitative estimation of which requires more careful study and is beyond scope of this paper. On the other hand our results of LL, NLL+NLO+v^2 in figure 4 is lower in its value and smaller in uncertainty partially due to this update.

---

[9]We do not include relatively small uncertainties from $\overline{\mathrm{MS}}$ mass ($\pm 2\%$) and from higher-order electroweak corrections.

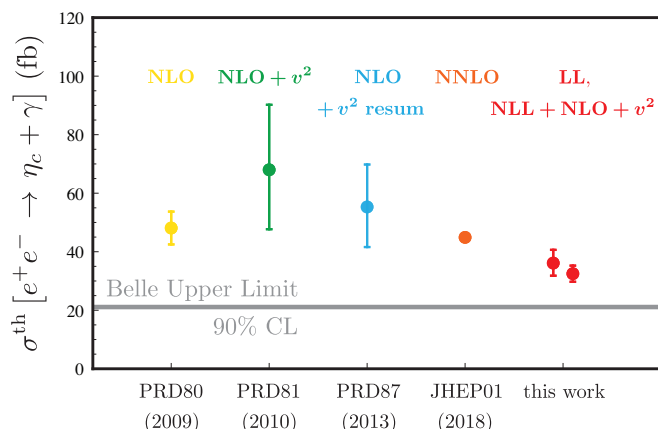**Figure 4**. Status of NRQCD predictions (points) and Belle's upper limit [30] (horizontal gray line) for $e^+e^- \to \eta_c + \gamma$. This work on right side for LL and for NLL+NLO with v^2 corrections is compared to previous predictions (from the left) at NLO [19], NLO with v^2 correction [17] and with v^2 resummation [22], and NNLO [21]. We note that uncertainties of NLO [19] and of NNLO [21] include only quark mass variations while the others include other sources of uncertainties. See the text for more details.

There are differences in scale choice and its variation. We use two scales $\mu = \sqrt{s}$ for the hard-scattering kernel and $\mu_0 = 2\overline{m}_c$ for the LCDA and decay constant and they are varied by a factor of 2 for μ and $\sqrt{2}$ for μ_0 as discussed in previous section. While we use $\overline{\text{MS}}$ mass $\overline{m}_c = 1.275^{+0.25}_{-0.35}$, many of previous results use the pole mass $m_c = 1.4 \sim 1.6$ GeV. NLO [19] sets $\mu = 2m_c$ and NLO+v^2 resummation [22] sets $\mu = m_c, 2m_c$ (result with $2m_c$ is shown in figure 4 and the value for m_c is similar), while NLO+v^2 [17] makes most conservative choice $\mu = \sqrt{s}, 2m_c$, and m_c, which leads to relatively larger uncertainty compared that of NLO+v^2 resummation. NNLO [21] chooses different values for renormalization scale $\mu_r = \sqrt{s}/2$ and the factorization scale $\mu_\Lambda = 1.0$ GeV. We do not include the result of [18] because the 1-loop coefficient is not consistent with other results [14, 17].

Recently the Belle experiment analyzed S-wave ($\eta_c + \gamma$) and P-wave ($\chi_{cJ} + \gamma$ with $J = 0, 1, 2$) channels [30]. While P-wave cross section ($J = 1$) and upper limits ($J = 0, 2$) are consistent with the theoretical predictions [16–19], S-wave upper limit $\sigma^{\text{exp}}_{\eta_c+\gamma} \leq 21.1$ fb at 90 % credibility level is in tension with our NLL+NLO prediction 32.7 ± 2.8 fb by 4.1σ. This reminds us the puzzle in exclusive $J/\psi + \eta_c$ production [56–59], where a large discrepancy between theory and experiment was resolved by the combined effect of large K-factor, resummed relativistic corrections and careful determination of NRQCD matrix element [51, 60–62].[10] However, in our case effect of the K-factor, a ratio of NLL+NLO including relativistic correction relative to LO, is less than 5% as shown in figure 1. It would be surprising if higher-order resummation or relativistic corrections is the resolution to this tension. Of course, more careful study on those corrections and other contributions from different topology can shed lights on the tension. Without correct understanding of this channel one may also cast a doubt on theoretical prediction for other exclusive

---

[10]Recently, [63] reports the K-factor (NNLO/LO) between +20% and -40% depending on scale choice.

processes such as radiative Higgs decay into quarkonium, a novel channel to probe the Yukawa coupling of charm quark [3, 4, 64, 65]. In this aspect, resolving the tension would be one of important checkpoints. The Belle II experiment with upgraded luminosity is starting its physics program and in a few years it will release improved measurements and can clarify if this seemingly tension is to be or not.

5 Summary

We resum large logarithms of $4m_Q^2/s$ at NLL accuracy for exclusive production for $\eta_{b,c} + \gamma$ in high-energy lepton colliders by using light-cone factorization theorem and by using 2-loop evolution kernel known from the pion form factor. The leading relativistic correction is also included and logarithms in the correction is resummed at LL accuracy. The nonsingular part of order α_s is obtained by subtracting the singular part from fixed-order results at NLO then, is added to resummed cross section. This makes our prediction of order α_s accuracy valid in both resummation region ($r \ll 1$) and fixed-order region ($r \sim O(1)$) where $r = 4m_Q^2/s$ such that the results with the same formalism in eq. (2.1) can be compared to measurement at the Belle energy near 10 GeV and in future colliders such as ILC, CEPC, FCC-ee.

Our final state $\eta_{c,b}$ is the pseudoscalar, which involves an ambiguity in handling γ_5 in d dimension and the scheme dependency enters in individual parts such as hard kernel, LCDA, and the decay constant in factorized formula. We explicitly showed that how the γ_5-scheme dependence vanishes in the resummed expression at NLL accuracy. In resummed expression, there is a part proportional to fixed-order singular result and its scheme independence is followed by that of the fixed-order cross section. In the other part of resummed expression, we observe that the scheme dependence of 2-loop anomalous dimension is matched to and cancelled against constant term of 1-loop hard-scattering kernel eq. (2.49).

In numerical calculation in section 3 we first rewrite the decay constant in terms of the experimental decay rate by eliminating NRQCD matrix element to avoid a systematic bias by unnecessary higher-order α_s contribution that can be contained in NRQCD matrix element. By doing this all the input formula are computed at the same α_s order to working accuracy and it is observed to show better perturbative convergence from LO to NLO and from LL to NLL. Our predictions for the cross sections and branching fraction are summarized in table 1. The input decay rates $\Gamma[\eta_{b,c} \to \gamma\gamma]$ dominates over the others including perturbative uncertainty and uncertainty of our prediction reduces if the measurement of decay rate improves. In section 4 we compare our prediction to previous predictions for the Belle experiment and discussed the differences in input parameters and uncertainty estimates. We also find Belle's recent upper limit 21 fb is about $4\,\sigma$ away from our prediction 33 ± 3 fb. We hope future Belle II analysis with better statistics coming-out in a few years and careful theoretical investigation on higher-order corrections may shed lights on this tension.

Acknowledgments

A   Fixed-order cross section

The fixed-order cross section up to $O(\alpha_s, v^2)$ was computed in [17]

$$\sigma^{\text{fixed}}(r; \mu) = \sigma_0 \left[(1 - r) + \frac{\alpha_s C_F}{4\pi} c^{\text{fixed}} + \langle v^2 \rangle c_{v^2}^{\text{fixed}} \right], \qquad (A.1)$$

where the coefficients c^{fixed} and $c_{v^2}^{\text{fixed}}$ are

$$
\begin{aligned}
c^{\text{fixed}} =& -\frac{2 \left[30r^2 - (84 + \pi^2)r + 2\pi^2 + 54 \right]}{3(2 - r)} + \frac{8(2r - 3)(1 - r)}{(2 - r)^2} \log\left(\frac{2}{r} - 2 \right) \\
& -\frac{12(1 - r)}{\sqrt{1 - r}} \log\left(\frac{1 - \sqrt{1 - r}}{1 + \sqrt{1 - r}} \right) - 2 \left[\left(1 + \frac{r}{2} \right) \log^2\left(\frac{1 - \sqrt{1 - r}}{1 + \sqrt{1 - r}} \right) - \log^2\left(\frac{2}{r} - 1 \right) \right] \\
& +4\text{Li}_2\left(\frac{r}{2 - r} \right), \\
c_{v^2}^{\text{fixed}} =& -\frac{4}{3}\left(1 - \frac{r}{4} \right).
\end{aligned}
\qquad (A.2)
$$

Note that our coefficient c^{fixed} is related to that of $C(r)$ in [17] as: $c^{\text{fixed}} = 3(1 - r)C(r)$.

B   Plus distributions

Here, we give the definition of plus distributions used in the paper. The $+$ and $++$ functions are defined by

$$
\begin{aligned}
\int_0^1 dx\, [f(x)]_+ g(x) &= \int_0^1 dx\, f(x)[g(x) - g(1/2)], \\
\int_0^1 dx\, [f(x)]_{++} g(x) &= \int_0^1 dx\, f(x)[g(x) - g(1/2) - g'(1/2)(x - 1/2)],
\end{aligned}
\qquad (B.1)
$$

The plus distribution depending on two arguments x and y is defined by

$$[f(x, y)]_+ \equiv f(x, y) - \delta(x - y) \int_0^1 dz f(z, y). \qquad (B.2)$$

C Anomalous dimension

The NLO anomalous dimension $\gamma_{n-1}^{\parallel(1)}$ is given in ref. [66] as

$$
\gamma_{n-1}^{(1)} = \left(C_F^2 - \frac{1}{2}C_F C_A \right) \left\{ 16 H_n \frac{2n+1}{n^2(n+1)^2} + 16\left[2H_n - \frac{1}{n(n+1)} \right]\left(H_n^{(2)} - S_{n/2}^{'(2)} \right) \right.
$$

$$
\left. + 64\tilde{S}_n + 24H_n^{(2)} - 3 - 8S_{n/2}^{'(3)} - 8\frac{3n^3+n^2-1}{n^3(n+1)^3} - 16(-1)^n\frac{2n^2+2n+1}{n^3(n+1)^3} \right\}
$$

$$
+ C_F C_A \left\{ H_n\left[\frac{536}{9} + 8\frac{2n+1}{n^2(n+1)^2} \right] - 16H_nH_n^{(2)} + H_n^{(2)}\left[-\frac{52}{3} + \frac{8}{n(n+1)} \right] \right.
$$

$$
\left. - \frac{43}{6} - 4\frac{151n^4+263n^3+97n^2+3n+9}{9n^3(n+1)^3} \right\}
$$

$$
+ C_F \frac{n_f}{2} \left\{ -\frac{160}{9}H_n + \frac{32}{3}H_n^{(2)} + \frac{4}{3} + 16\frac{11n^2+5n-3}{9n^2(n+1)^2} \right\}, \tag{C.1}
$$

where

$$
H_n^{(k)} \equiv \sum_{j=1}^n \frac{1}{j^k}, \quad \text{with} \quad H_n^{(1)} \equiv H_n, \tag{C.2}
$$

$$
S_{n/2}^{'(k)} \equiv \begin{cases} H_{n/2}^{(k)}, & \text{if } n \text{ is even}, \\ H_{(n-1)/2}^{(k)}, & \text{if } n \text{ is odd}, \end{cases} \tag{C.3}
$$

$$
\tilde{S}_n \equiv \sum_{j=1}^n \frac{(-1)^j}{j^2}H_j. \tag{C.4}
$$

The off-diagonal evolution factor $d_{nk}(\mu,\mu_0)$ is given by

$$
d_{nk}(\mu,\mu_0) = \frac{M_{nk}}{\gamma_n^{(0)} - \gamma_k^{(0)} - 2\beta_0} \left\{ 1 - \left[\frac{\alpha_s(\mu)}{\alpha_s(\mu_0)} \right]^{\frac{\gamma_n^{(0)} - \gamma_k^{(0)} - 2\beta_0}{2\beta_0}} \right\}, \tag{C.5}
$$

where

$$
M_{nk} = \frac{(k+1)(k+2)(k+3)}{(n+1)(n+2)}(\gamma_n^{(0)} - \gamma_k^{(0)})
$$

$$
\times \left[\frac{8C_F A_{nk} - \gamma_k^{(0)} - 2\beta_0}{(n-k)(n+k+3)} + 4C_F\frac{A_{nk} - \psi(n+2) + \psi(1)}{(k+1)(k+2)} \right],
$$

$$
A_{nk} = \psi\left(\frac{n+k+4}{2} \right) - \psi\left(\frac{n-k}{2} \right) + 2\psi(n-k) - \psi(n+2) - \psi(1), \tag{C.6}
$$

and $\psi(n)$ is the digamma function.

References

[1] G.T. Bodwin, E. Braaten, E. Eichten, S.L. Olsen, T.K. Pedlar and J. Russ, *Quarkonium at the frontiers of high energy physics: a Snowmass white paper*, in *Proceedings*, 2013 *Community Summer Study on the Future of U.S. Particle Physics: Snowmass on the Mississippi (CSS*2013*)*, Minneapolis, MN, U.S.A., 29 July–6 August 2013 [arXiv:1307.7425] [INSPIRE].

[2] A. Andronic et al., *Heavy-flavour and quarkonium production in the LHC era: from proton-proton to heavy-ion collisions*, *Eur. Phys. J.* **C 76** (2016) 107 [arXiv:1506.03981] [INSPIRE].

[3] CMS collaboration, *Search for rare decays of Z and Higgs bosons to J/ψ and a photon in proton-proton collisions at $\sqrt{s} = 13$ TeV*, *Eur. Phys. J.* **C 79** (2019) 94 [arXiv:1810.10056] [INSPIRE].

[4] ATLAS collaboration, *Searches for exclusive Higgs and Z boson decays into J/ψγ, ψ(2S)γ and Υ(nS)γ at $\sqrt{s} = 13$ TeV with the ATLAS detector*, *Phys. Lett.* **B 786** (2018) 134 [arXiv:1807.00802] [INSPIRE].

[5] G.T. Bodwin, E. Braaten and G.P. Lepage, *Rigorous QCD analysis of inclusive annihilation and production of heavy quarkonium*, *Phys. Rev.* **D 51** (1995) 1125 [*Erratum ibid.* **D 55** (1997) 5853] [hep-ph/9407339] [INSPIRE].

[6] T. Behnke et al., *The International Linear Collider technical design report — volume* 1: *executive summary*, arXiv:1306.6327 [INSPIRE].

[7] CEPC STUDY GROUP collaboration, *CEPC conceptual design report: volume* 2 *— physics & detector*, arXiv:1811.10545 [INSPIRE].

[8] TLEP DESIGN STUDY WORKING GROUP collaboration, *First look at the physics case of TLEP*, *JHEP* **01** (2014) 164 [arXiv:1308.6176] [INSPIRE].

[9] G.P. Lepage and S.J. Brodsky, *Exclusive processes in perturbative quantum chromodynamics*, *Phys. Rev.* **D 22** (1980) 2157 [INSPIRE].

[10] V.L. Chernyak and A.R. Zhitnitsky, *Asymptotic behavior of exclusive processes in QCD*, *Phys. Rept.* **112** (1984) 173 [INSPIRE].

[11] C.W. Bauer, S. Fleming, D. Pirjol, I.Z. Rothstein and I.W. Stewart, *Hard scattering factorization from effective field theory*, *Phys. Rev.* **D 66** (2002) 014017 [hep-ph/0202088] [INSPIRE].

[12] Y. Jia and D. Yang, *Refactorizing NRQCD short-distance coefficients in exclusive quarkonium production*, *Nucl. Phys.* **B 814** (2009) 217 [arXiv:0812.1965] [INSPIRE].

[13] Y. Jia, J.-X. Wang and D. Yang, *Bridging light-cone and NRQCD approaches: asymptotic behavior of B_c electromagnetic form factor*, *JHEP* **10** (2011) 105 [arXiv:1012.6007] [INSPIRE].

[14] X.-P. Wang and D. Yang, *The leading twist light-cone distribution amplitudes for the S-wave and P-wave quarkonia and their applications in single quarkonium exclusive productions*, *JHEP* **06** (2014) 121 [arXiv:1401.0122] [INSPIRE].

[15] G. Bell and T. Feldmann, *Modelling light-cone distribution amplitudes from non-relativistic bound states*, *JHEP* **04** (2008) 061 [arXiv:0802.2221] [INSPIRE].

[16] H.S. Chung, J. Lee and C. Yu, *Exclusive heavy quarkonium + γ production from e^+e^- annihilation into a virtual photon*, *Phys. Rev.* **D 78** (2008) 074022 [arXiv:0808.1625] [INSPIRE].

[17] W.-L. Sang and Y.-Q. Chen, *Higher order corrections to the cross section of $e^+e^- \to$ quarkonium + γ*, *Phys. Rev.* **D 81** (2010) 034028 [arXiv:0910.4071] [INSPIRE].

[18] V.V. Braguta, *Exclusive C = + charmonium production in $e^+e^- \to H + \gamma$ at B-factories within light cone formalism*, *Phys. Rev.* **D 82** (2010) 074009 [arXiv:1006.5798] [INSPIRE].

[19] D. Li, Z.-G. He and K.-T. Chao, *Search for C = + charmonium and bottomonium states in $e^+e^- \to \gamma + X$ at B factories*, *Phys. Rev.* **D 80** (2009) 114014 [arXiv:0910.4155] [INSPIRE].

[20] F. Feng, Y. Jia and W.-L. Sang, *Can nonrelativistic QCD explain the $\gamma\gamma^* \to \eta_c$ transition form factor data?*, *Phys. Rev. Lett.* **115** (2015) 222001 [arXiv:1505.02665] [INSPIRE].

[21] L.-B. Chen, Y. Liang and C.-F. Qiao, *NNLO QCD corrections to $\gamma + \eta_c(\eta_b)$ exclusive production in electron-positron collision*, *JHEP* **01** (2018) 091 [arXiv:1710.07865] [INSPIRE].

[22] Y. Fan, J. Lee and C. Yu, *Resummation of relativistic corrections to exclusive productions of charmonia in e^+e^- collisions*, *Phys. Rev.* **D 87** (2013) 094032 [arXiv:1211.4111] [INSPIRE].

[23] G.-Z. Xu, Y.-J. Li, K.-Y. Liu and Y.-J. Zhang, *$\alpha_s v^2$ corrections to η_c and χ_{cJ} production recoiled with a photon at e^+e^- colliders*, *JHEP* **10** (2014) 071 [arXiv:1407.3783] [INSPIRE].

[24] G. Chen, X.-G. Wu, Z. Sun, S.-Q. Wang and J.-M. Shen, *Exclusive charmonium production from e^+e^- annihilation round the Z^0 peak*, *Phys. Rev.* **D 88** (2013) 074021 [arXiv:1308.5375] [INSPIRE].

[25] G. Chen, X.-G. Wu, Z. Sun, X.-C. Zheng and J.-M. Shen, *Next-to-leading order QCD corrections for the charmonium production via the channel $e^+e^- \to H(|c\bar{c}\rangle) + \gamma$ round the Z^0 peak*, *Phys. Rev.* **D 89** (2014) 014006 [arXiv:1311.2735] [INSPIRE].

[26] G.T. Bodwin, H.S. Chung, J.-H. Ee, J. Lee and F. Petriello, *Relativistic corrections to Higgs boson decays to quarkonia*, *Phys. Rev.* **D 90** (2014) 113010 [arXiv:1407.6695] [INSPIRE].

[27] G.T. Bodwin, H.S. Chung, J.-H. Ee and J. Lee, *New approach to the resummation of logarithms in Higgs-boson decays to a vector quarkonium plus a photon*, *Phys. Rev.* **D 95** (2017) 054018 [arXiv:1603.06793] [INSPIRE].

[28] G.T. Bodwin, H.S. Chung, J.-H. Ee and J. Lee, *Addendum: new approach to the resummation of logarithms in Higgs-boson decays to a vector quarkonium plus a photon*, *Phys. Rev.* **D 96** (2017) 116014 [arXiv:1710.09872] [INSPIRE].

[29] G.T. Bodwin, H.S. Chung, J.-H. Ee and J. Lee, *Z-boson decays to a vector quarkonium plus a photon*, *Phys. Rev.* **D 97** (2018) 016009 [arXiv:1709.09320] [INSPIRE].

[30] BELLE collaboration, *Observation of $e^+e^- \to \gamma\chi_{c1}$ and search for $e^+e^- \to \gamma\chi_{c0}, \gamma\chi_{c2}$, and $\gamma\eta_c$ at $\sqrt{s}$ near $10.6\,GeV$ at Belle*, *Phys. Rev.* **D 98** (2018) 092015 [arXiv:1810.10291] [INSPIRE].

[31] D. Kang, C. Lee and I.W. Stewart, *Using 1-jettiness to measure 2 jets in DIS 3 ways*, *Phys. Rev.* **D 88** (2013) 054004 [arXiv:1303.6952] [INSPIRE].

[32] D. Kang, C. Lee and I.W. Stewart, *Analytic calculation of 1-jettiness in DIS at $\mathcal{O}(\alpha_s)$*, *JHEP* **11** (2014) 132 [arXiv:1407.6706] [INSPIRE].

[33] E. Braaten, *QCD corrections to meson-photon transition form-factors*, *Phys. Rev.* **D 28** (1983) 524 [INSPIRE].

[34] M.S. Chanowitz, M. Furman and I. Hinchliffe, *The axial current in dimensional regularization*, *Nucl. Phys.* **B 159** (1979) 225 [INSPIRE].

[35] G. 't Hooft and M.J.G. Veltman, *Regularization and renormalization of gauge fields*, *Nucl. Phys.* **B 44** (1972) 189 [INSPIRE].

[36] P. Breitenlohner and D. Maison, *Dimensional renormalization and the action principle*, *Commun. Math. Phys.* **52** (1977) 11 [INSPIRE].

[37] W. Wang, J. Xu, D. Yang and S. Zhao, *Relativistic corrections to light-cone distribution amplitudes of S-wave B_c mesons and heavy quarkonia*, *JHEP* **12** (2017) 012 [arXiv:1706.06241] [INSPIRE].

[38] G.T. Bodwin and Y.-Q. Chen, *Renormalon ambiguities in NRQCD operator matrix elements*, *Phys. Rev.* **D 60** (1999) 054008 [hep-ph/9807492] [INSPIRE].

[39] R. Tarrach, *The pole mass in perturbative QCD*, *Nucl. Phys.* **B 183** (1981) 384 [INSPIRE].

[40] A.V. Efremov and A.V. Radyushkin, *Factorization and asymptotical behavior of pion form-factor in QCD*, *Phys. Lett.* **B 94** (1980) 245 [INSPIRE].

[41] F.M. Dittes and A.V. Radyushkin, *Two loop contribution to the evolution of the pion wave function*, *Phys. Lett.* **B 134** (1984) 359 [INSPIRE].

[42] M.H. Sarmadi, *The asymptotic pion form-factor beyond the leading order*, *Phys. Lett.* **B 143** (1984) 471 [INSPIRE].

[43] S.V. Mikhailov and A.V. Radyushkin, *Evolution kernels in QCD: two loop calculation in Feynman gauge*, *Nucl. Phys.* **B 254** (1985) 89 [INSPIRE].

[44] G.R. Katz, *Two loop Feynman gauge calculation of the meson nonsinglet evolution potential*, *Phys. Rev.* **D 31** (1985) 652 [INSPIRE].

[45] G.W. Jones, *Meson distribution amplitudes — applications to weak radiative B decays and B transition form factors*, Ph.D. thesis, Durham U., Durham, U.K. (2007) [arXiv:0710.4479] [INSPIRE].

[46] S.S. Agaev, V.M. Braun, N. Offen and F.A. Porkert, *Light cone sum rules for the $\pi^0\gamma^*\gamma$ form factor revisited*, *Phys. Rev.* **D 83** (2011) 054020 [arXiv:1012.4671] [INSPIRE].

[47] B. Melic, B. Nizic and K. Passek, *BLM scale setting for the pion transition form-factor*, *Phys. Rev.* **D 65** (2002) 053020 [hep-ph/0107295] [INSPIRE].

[48] J. Erler, *Calculation of the QED coupling $\alpha(M_Z)$ in the modified minimal subtraction scheme*, *Phys. Rev.* **D 59** (1999) 054008 [hep-ph/9803453] [INSPIRE].

[49] J. Erler, *Global fits to electroweak data using GAPP*, in *QCD and weak boson physics in run II. Proceedings*, Batavia, IL, U.S.A. 4–6 March, 3–4 June, 4–6 November 1999 [hep-ph/0005084] [INSPIRE].

[50] T. van Ritbergen, J.A.M. Vermaseren and S.A. Larin, *The four loop β-function in quantum chromodynamics*, *Phys. Lett.* **B 400** (1997) 379 [hep-ph/9701390] [INSPIRE].

[51] G.T. Bodwin, H.S. Chung, D. Kang, J. Lee and C. Yu, *Improved determination of color-singlet nonrelativistic QCD matrix elements for S-wave charmonium*, *Phys. Rev.* **D 77** (2008) 094017 [arXiv:0710.0994] [INSPIRE].

[52] PARTICLE DATA GROUP collaboration, *Review of particle physics*, *Phys. Rev.* **D 98** (2018) 030001 [INSPIRE].

[53] H.S. Chung, J. Lee and C. Yu, *NRQCD matrix elements for S-wave bottomonia and* $\Gamma[\eta_b(nS) \to \gamma\gamma]$ *with relativistic corrections*, *Phys. Lett.* **B 697** (2011) 48 [arXiv:1011.1554] [INSPIRE].

[54] G.T. Bodwin, D. Kang and J. Lee, *Potential-model calculation of an order-v^2 NRQCD matrix element*, *Phys. Rev.* **D 74** (2006) 014014 [hep-ph/0603186] [INSPIRE].

[55] J.-Z. Li, Y.-Q. Ma and K.-T. Chao, *QCD and relativistic $O(\alpha_s v^2)$ corrections to hadronic decays of spin-singlet heavy quarkonia h_c, h_b and η_b*, *Phys. Rev.* **D 88** (2013) 034002 [arXiv:1209.4011] [INSPIRE].

[56] BELLE collaboration, *Study of double charmonium production in e^+e^- annihilation at* $\sqrt{s} \sim 10.6\,GeV$, *Phys. Rev.* **D 70** (2004) 071102 [hep-ex/0407009] [INSPIRE].

[57] BABAR collaboration, *Measurement of double charmonium production in e^+e^- annihilations at* $\sqrt{s} = 10.6\,GeV$, *Phys. Rev.* **D 72** (2005) 031101 [hep-ex/0506062] [INSPIRE].

[58] E. Braaten and J. Lee, *Exclusive double charmonium production from e^+e^- annihilation into a virtual photon*, *Phys. Rev.* **D 67** (2003) 054007 [*Erratum ibid.* **D 72** (2005) 099901] [hep-ph/0211085] [INSPIRE].

[59] K.-Y. Liu, Z.-G. He and K.-T. Chao, *Problems of double charm production in e^+e^- annihilation at* $\sqrt{s} = 10.6\,GeV$, *Phys. Lett.* **B 557** (2003) 45 [hep-ph/0211181] [INSPIRE].

[60] Y.-J. Zhang, Y.-J. Gao and K.-T. Chao, *Next-to-leading order QCD correction to* $e^+e^- J/\psi + \eta_c$ *at* $\sqrt{s} = 10.6\,GeV$, *Phys. Rev. Lett.* **96** (2006) 092001 [hep-ph/0506076] [INSPIRE].

[61] G.T. Bodwin, J. Lee and C. Yu, *Resummation of relativistic corrections to $e^+e^- \to J/\psi + \eta_c$*, *Phys. Rev.* **D 77** (2008) 094018 [arXiv:0710.0995] [INSPIRE].

[62] Z.-G. He, Y. Fan and K.-T. Chao, *Relativistic corrections to J/ψ exclusive and inclusive double charm production at B factories*, *Phys. Rev.* **D 75** (2007) 074011 [hep-ph/0702239] [INSPIRE].

[63] F. Feng, Y. Jia and W.-L. Sang, *Next-to-next-to-leading-order QCD corrections to* $e^+e^- \to J/\psi + \eta_c$ *at B factories*, arXiv:1901.08447 [INSPIRE].

[64] G.T. Bodwin, F. Petriello, S. Stoynev and M. Velasco, *Higgs boson decays to quarkonia and the $H\bar{c}c$ coupling*, *Phys. Rev.* **D 88** (2013) 053003 [arXiv:1306.5770] [INSPIRE].

[65] S. Mao, Y. Guo-He, L. Gang, Z. Yu and G. Jian-You, *Probing the charm-Higgs Yukawa coupling via Higgs boson decay to h_c plus a photon*, *J. Phys.* **G 46** (2019) 105008 [arXiv:1905.01589] [INSPIRE].

[66] A. Gonzalez-Arroyo, C. Lopez and F.J. Yndurain, *Second order contributions to the structure functions in deep inelastic scattering. 1. Theoretical calculations*, *Nucl. Phys.* **B 153** (1979) 161 [INSPIRE].